

# We are IntechOpen, the world's leading publisher of Open Access books Built by scientists, for scientists

**4,800**

Open access books available

**122,000**

International authors and editors

**135M**

Downloads

Our authors are among the

**154**

Countries delivered to

**TOP 1%**

most cited scientists

**12.2%**

Contributors from top 500 universities



**WEB OF SCIENCE™**

Selection of our books indexed in the Book Citation Index  
in Web of Science™ Core Collection (BKCI)

Interested in publishing with us?  
Contact [book.department@intechopen.com](mailto:book.department@intechopen.com)

Numbers displayed above are based on latest data collected.

For more information visit [www.intechopen.com](http://www.intechopen.com)



# Hot Forming Characteristics of Magnesium Alloy AZ31 and Three-Dimensional FE Modeling and Simulation of the Hot Splitting Spinning Process

He Yang<sup>1</sup>, Liang Huang and Mei Zhan

*State Key Laboratory of Solidification Processing, School of Materials Science and Engineering, Northwestern Polytechnical University, P.O.Box 542, Xi'an, 710072, China*

## 1. Introduction

As one kind of lightweight alloys in the widely applications, magnesium alloys are currently the lightest structural materials with low density, high specific strength and specific stiffness, superior damping capacity [Michael et al., 1999; Mordike & Ebert, 2001]. The superior damping capacity is provided by the lower Young's modulus-E, and the value of E is no sensitive to material microstructures. When a structural component of magnesium alloy is subject to the same impact loadings, it can perform more elastic deformation and absorb more impact energy. Besides, stress distributions inside of a structural component of magnesium alloy are more uniform, thereby high stress concentrations can be avoided. Therefore, a structural component of magnesium alloy subjected to the impact loadings can be formed. Meanwhile, as one new continuous and local plastic forming technology, splitting spinning is designed to split a revolving disk blank from the outer rectangular edge into two flanges using a roller called splitting roller with a sharp corner, and then shaping spinning is done by two or three other forming rollers [Wong et al., 2003; Wang & Liu, 1986], as shown in Fig. 1. Compared with other conventional methods combining with casting, forging and welding and then mechanical processing, splitting spinning has the remarkable advantages of high efficiency, low cost and good flexibility, and its products for aeronautics, astronautics, automobile and weapon industry meet the high quality and high precision demands and are developed at low costs in a short time [Yang et al., 2004; Song et al., 2000]. Accordingly, based on the above remarkable advantages and application foregrounds of magnesium alloy AZ31 and the above manufacturing predominance of splitting spinning, a structure component of magnesium alloy AZ31 subjected to the impact loadings and with high quality and high precision can be formed using splitting spinning, such as, a wheel hub of aero undercarriage or kinds of light whole wheels.

According to the past research on deformation property of magnesium alloy, the ductility and formability of magnesium alloy is low at room temperature due to its hexagonal close-

---

<sup>1</sup> E-mail: yanghe@nwpu.edu.cn

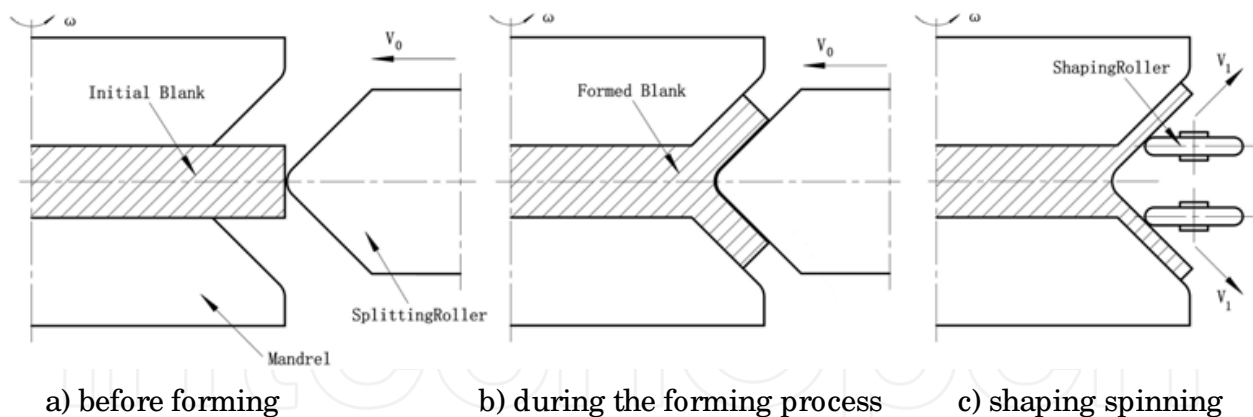


Fig. 1. Schematic illustration of splitting spinning

packed (HCP) crystal structure, so it is difficult to be deformed. However, it shows excellent ductility and formability at elevated temperatures. Especially, magnesium alloy AZ31 is characterized by a good formability and ductility at elevated temperature [Palumbo et al., 2007]. The investigation by Ogawa et al. [Ogawa et al., 2002] indicated that the determination of appropriate forming temperature of magnesium alloy AZ31 is one of key factors, thereby the forming limit is improved and the fracture of specimen is avoided. The investigation by Doege et al. [Doege & Droder, 2001] indicated that high forming limit of magnesium alloy AZ31 could be obtained when the forming temperature exceeds 200°C, on the contrary, forming limit reduced and forming quality of a structural component decreased when forming temperature reaches above 450°C. Consequently, many recent research activities show that, magnesium alloy AZ31 has the features of the high plastic formability from 200°C to 450°C, and it can be deformed into a desired structural component.

Due to the limitation of experimental study and theoretical analysis, the investigations on the distributions of stress, strain and temperature and the influencing laws of forming parameters on forming quality are difficulties during metal forming processes. FE numerical simulation is applied increasingly and is becoming a very important tool for the research on the field distributions and forming quality of a structural component [Grass et al., 2003; Grass et al., 2006]. At present, there are only some research on the FE numerical simulations of splitting spinning. Based on the FE software DEFORM2D V5.02 and MARC/ Autoforge V1.2, Hauk et al. [Hauk et al., 2000] studied the forming characteristics and rules of splitting spinning using elastic-plastic FEM, and the mechanism and laws of geometric dimensions of disk blank and friction influencing on deformation during the process are obtained under the two-dimensional space. And then experimental research are performed by means of the equipments called Tooling System, the influencing laws of different materials, different feed rates and different splitting spinning angles on splitting spinning force during the process are obtained [Schmoeckel & Hauk, 2000]. The deviation between two-dimensional simulation data and experiment data is acceptable, so the results are usable. Nevertheless, the 3D FE model reduced disk blank, simplified feeding mechanism system and ignored friction action between disk blank and supporting roller during the forming process in order to reduce computational time and improve computational efficiency. So, the above assumptions resulted in lower computational precision, such as, the splitting spinning force in simulations was less than the one in experiments, about one half. So in order to obtain more accurate simulation results, a reliable and practical 3D FE model of splitting spinning should be established.

The authors have studied the cold splitting spinning process of aluminium alloy. A reliable and practical 3D-FE model of cold splitting spinning of aluminium alloy is established, and

the variations of spinning force, stress fields and strain fields with time are obtained [Huang<sup>1</sup> et al., 2008]. The influencing laws of forming parameters of splitting spinning on the quality and precision of flanges are investigated based on the forming characteristics of splitting spinning combining with the behaviors of roller [Huang et al., 2009]. The influencing laws of material parameters on splitting spinning force, splitting spinning moment and forming quality of flange have been investigated [Huang<sup>2</sup> et al., 2008]. A reliable theoretical model established by the principal stress method is proposed for the calculation of splitting spinning force, and the influencing laws of forming parameters on splitting spinning force are investigated [Huang<sup>3</sup> et al., 2008]. However, the research on hot splitting spinning of magnesium alloy AZ31 is scant by now, so the above results may help study hot splitting spinning of magnesium alloy AZ31.

In this paper, according to the analysis of microstructures and deformation characteristics of magnesium alloy AZ31, the reasonable forming temperature range is obtained during the thermoplastic forming process. A three-dimensional elastic-plastic FE model of hot splitting spinning of magnesium alloy AZ31 is established based on the FEM software platform of ABAQUS/ Explicit and a developed three-dimensional FE model of cold splitting spinning, and then the reliability is verified by theoretical evaluation. The modeling procedures are summarized, the comparisons of the modeling process between hot splitting spinning and traditional spinning are presented, and some key technologies are proposed. Adopting the FE model, field distributions of deformed component, including temperature fields, stress fields and strain fields, and variations of different nodal temperature are obtained, and the influencing laws of different initial temperatures of disk blank and different feed rates of splitting roller on the forming quality and precision of deformed flanges are investigated, consequently the optimal forming temperature and the optimal feed rate of splitting roller during the hot splitting spinning process of magnesium alloy AZ31 are obtained.

## 2. Hot forming characteristics of magnesium alloy AZ31

The deformation mechanisms of magnesium alloy mainly contain twinning and slip, and deformation texture roots in basal slips among grain boundaries [Staroselsky & Anand, 2003; Chino<sup>1</sup> et al., 2008; Chino<sup>2</sup> et al., 2008]. All these deformation mechanisms and texture characteristics affect plastic deformation behaviors, formability and mechanical property of magnesium alloy strongly. During the hot splitting spinning process, magnesium alloy AZ31 (Mg-3mass%Al-1%massZn-0.5%massMn) disk blank is mainly extruded, so microstructures of the extrusion specimen for different forming temperatures must be realized in order to obtain the optimal forming temperature range and forming parameters. Thermal mechanical property of magnesium alloy AZ31 is quite related to processing technology, heat treatment process and so on, especially for different forming temperatures, thermal mechanical property of magnesium alloy AZ31 varies on a large scope. Therefore, according to the analysis of microstructures and deformation characteristics of magnesium alloy AZ31, hot forming characteristics are obtained. And then the forming rules during the hot splitting spinning process of magnesium alloy AZ31 under tensile stress and compressive stress simultaneously is revealed and the optimal forming parameters and forming temperature range are obtained.

According to excellent ductility and formability of magnesium alloy AZ31 at elevated temperatures and forming temperature variation from 200°C to 450°C, there are two kinds of specimen [Chino<sup>2</sup> et al., 2008], which are the extrusion magnesium alloy AZ31 processed by

extruding at 500°C is called the sample A (above the high temperature variation ) and the extrusion magnesium alloy AZ31 processed by extruding at 210°C is called the sample B (within high temperature variation). Fig. 2 is shown as microstructure of magnesium alloy AZ31 specimen, (a) sample A and (b) sample B. Usually, the plasticity or ductility of magnesium alloy AZ31 is low at room temperature, but at elevated temperatures, plastic deformation energy is activated among grains and grain boundaries, so the plasticity and forming limit are improved. For magnesium alloy AZ31, forming temperature must be controlled from 200°C to 450°C. Because plastic deformation energy is inactivated among grains and grain boundaries below 200°C, and disk blank of magnesium alloy AZ31 may brittle fracture easily, nevertheless, when temperature is above 450°C, disk blank of magnesium alloy AZ31 may be oxide etch and grain size may become large, even phase transformation arises and plasticity decreases, as shown in Fig. 2(a). According to Fig. 2, it can be found that, microstructure of sample A shows large grain size obviously and the average grain size is 71  $\mu m$  for sample A, and microstructure of sample B shows close and small grain size and the average grain size is 8  $\mu m$  for sample B.

According to the above analysis of microstructures, the twin interfaces energy of magnesium alloy AZ31 is significantly large and twin nucleation decreases with decreasing grain size. The plasticity and formability of magnesium alloy AZ31 is low and the response of plastic deformation is inadequacy below 200°C. But when magnesium alloy AZ31 is at elevated temperatures, the plastic deformation energy transforms internal energy and the forming process is done successfully and well, consequently the requirement of close and small grain size in a whole structural component is satisfied. Meanwhile, it is necessary to control the upper limit of forming temperature in order to avoid oxide etch and large grain size inside of the whole structural component of magnesium alloy AZ31, even phase transformation.

Furthermore, due to dynamic recovery (DRV) and dynamic recrystallization (DRX), deformation magnesium alloy shows distinct high temperature softening during the hot forming process. The strain softening is the typical characteristic of the elevated flow stress model of magnesium alloys, whose material response can principally be divided into two categories during the hot forming process, DRV type and DRX type. For magnesium alloy AZ31, DRX is the main characteristic of flow stress curves [Liu et al., 2008]. And also, the temperature of dynamic recrystallization (DRX) of magnesium alloy AZ31 is approximate from 533K to 593K [Liu et al., 2008].

According to the above microstructures and deformation characteristics of magnesium alloy AZ31 with the characteristics of homogeneous and isotropic elastic-plastic body, magnesium alloy AZ31 shows excellent ductility and plasticity when forming temperature ranges from 200 °C to 450°C. Therefore, plastic deformation mechanisms of magnesium alloy AZ31 and research foundations of hot splitting spinning of magnesium alloy AZ31 are obtained.

### 3. FE modeling process of hot splitting spinning of magnesium alloy AZ31

#### 3.1 Establishment of FE model of hot splitting spinning of magnesium alloy AZ31

During the hot splitting spinning process of magnesium alloy AZ31, two Mandrels rotate at a rotational speed of  $\omega$ , and SplittingRoller feeds at a linear speed of  $v$  in the radial

direction of Diskblank. Meanwhile, under the effects of the friction between Diskblank and SplittingRoller and the extrusions of two Mandrels, Diskblank is split into two flanges from the outer rectangular edge using SplittingRoller with a sharp corner, which come into the gaps at the joints between SplittingRoller and two Mandrels. After the forming ends, the radius of Diskblank reduces, and two flanges are produced. According to the forming characteristics of hot splitting spinning of magnesium alloy AZ31, Diskblank is defined as a 3D deformable solid body, SplittingRoller is defined as an analytical rigid body, and two Mandrels are defined as discrete rigid bodies. Each rigid body is assigned with a reference point (RP) to represent its rigid motion in all degrees of freedom. In materials Property module, the model gives the density, Young's modulus, Poisson's ratio, constitutive equations and some thermal constants to material Diskblank which is a homogeneous and isotropic elastic-plastic body, and the model follows von Mises yield criterion and shear friction model [Yu & Chen, 1999].

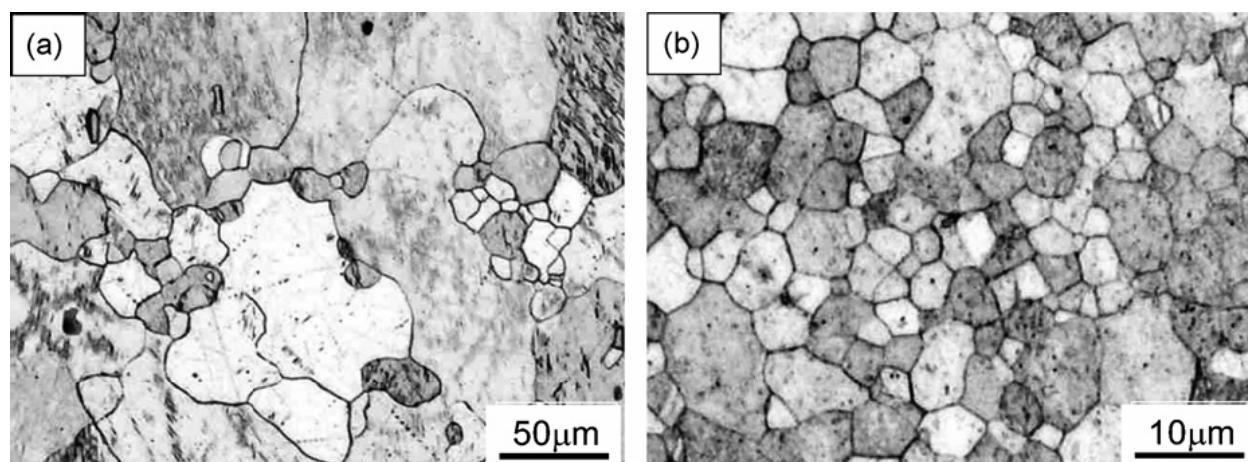


Fig. 2. Microstructure of magnesium alloy AZ31 extrusions, (a) sample A and (b) sample B [Chino<sup>2</sup> et al., 2008]

The heat transfer during the hot splitting spinning process of magnesium alloy AZ31 is a very complicated coupled thermo-mechanical problem. During the hot forming process, the free surface of disk blank exchanges heat with external environment by means of convection and radiation, and the contact surface conducts heat to the dies. Meanwhile, the plasticity deformation energy of disk blank is mostly converted into heat energy and internal energy. In order to define the thermal-dependent contacts among bodies and position them relative to each other in only one global coordinate system in which workpiece and dies would be identical with practical places during the hot forming process, some thermal-dependent contact surfaces and three thermal-dependent contact pairs are defined [Huang<sup>1</sup> et al., 2008]. The study arranges only one step called Splitting-Process in simulations, meanwhile, sets a suitable mass scaling factor in order to improve the computational efficiency. Moreover, here are the output requests, including Field output requests and History output requests, which contain stress, strain, displacement, force, temperature and energy of the whole model or special elements.

Consequently in this study, based on the FEM software platform of ABAQUS/ Explicit, a three-dimensional elastic-plastic FE model of hot splitting spinning of magnesium alloy AZ31 is established, as shown in Fig. 3.

### 3.2 Key technologies treatments during the modeling process

#### 3.2.1 Determination of exact forming time

During the 3D FE simulation process of hot splitting spinning of magnesium alloy AZ31, how to make sure the exact forming time is one of key factors which can exactly predict and control the hot forming process. Therefore, this study deduces a formula including velocity, displacement and time, as follows.

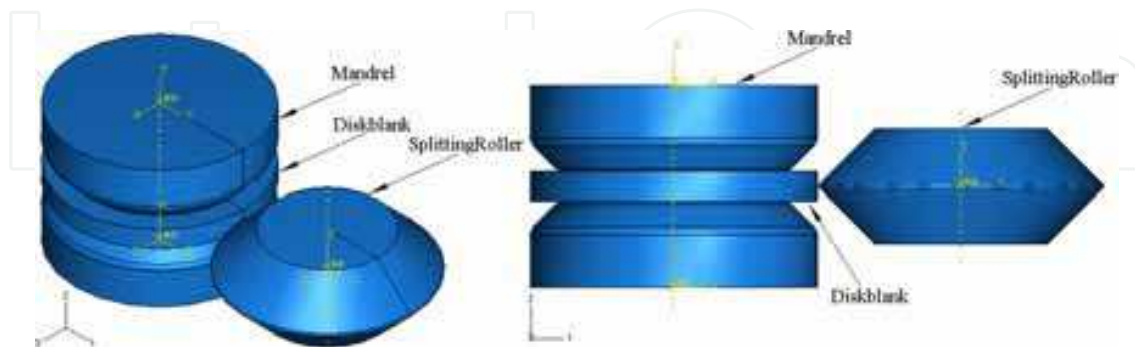


Fig. 3. Three-dimensional elastic-plastic FE model of hot splitting spinning of magnesium alloy AZ31 under ABAQUS/ Explicit.

It is shown as the exact forming time calculation of splitting spinning in Fig. 4. According to Fig. 4, the ending face  $\overline{A_1B_1}$  indicated by the thin broken lines before the forming translates to the ending face  $\overline{A_2B_2}$  indicated by the broad real lines after the forming. Therefore, along the feeding direction of SplittingRoller, a formula is given as,

$$L_0 = V_0 T \quad (1)$$

where  $L_0$  is the feed amount of SplittingRoller,  $V_0$  is the feed rate of SplittingRoller,  $T$  is the forming time. Similarly, along the other feeding direction, a formula is given as,

$$L_1 = V_1 T \quad (2)$$

where  $L_1$  is the other feed amount of SplittingRoller,  $V_1$  is the other feed rate of SplittingRoller. Meanwhile, according to velocity vector analysis in Fig. 4, we obtain that

$$\sin \alpha = \frac{V_1}{V_0} = \frac{L_1/T}{V_0} = \frac{L - t_0/2}{V_0 T} \quad (3)$$

And the displacement  $L$  is obtained by

$$L = S_0 \cos \alpha \sin \alpha + \frac{t_0}{2} \cos \alpha \quad (4)$$

Therefore, substitution of Eqs. (4) into Eq. (3), the forming time  $T$  is expressed by

$$T = \frac{2S_0 \cos \alpha \sin \alpha + t_0 \cos \alpha - t_0}{2V_0 \sin \alpha} \quad (5)$$

Due to the round corner of SplittingRoller sticking to circumferential surface of the workpiece, the actual feed amount of SplittingRoller is less than the displacement  $L_0$ , as shown in right enlarged view of Fig. 4. So the displacement  $\Delta L$  is obtained by

$$\Delta L = \frac{R}{\sin \alpha} - R \quad (6)$$

Therefore, the actual feed amount of Splitting Roller  $L'$  is expressed by

$$L' = L - \Delta L \quad (7)$$

According to Eqs. (4), (5), (6) and (7), the exact forming time of 3D FE model of splitting spinning after rearranging is given by

$$T = \frac{S_0 \cos \alpha \sin \alpha + \frac{t_0}{2} \cos \alpha + R \sin \alpha - R - \frac{t_0}{2}}{V_0 \sin \alpha} \quad (8)$$

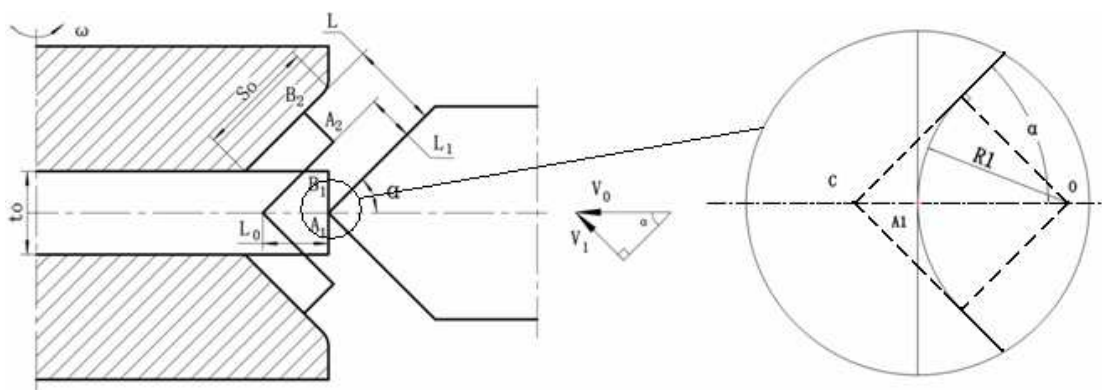


Fig. 4. Exact forming time calculation of splitting spinning

### 3.2.2 Determination of constitutive equations of magnesium alloy AZ31

Microstructures during the thermal plastic forming process reflects constitutive equations of thermal plastic deformation on the macroscopic view, namely, the flow stress model with the characteristics of temperature, strain rate, strain and microstructure evolution. It represents one basic variable during the hot forming process, and determines the loadings quantity and the required energy magnitude. The flow stress is affected not only by forming temperature, deformation degree, strain rate and chemical composition, but also by the microstructure evolution within deformation body.

The flow stress curves of magnesium alloy AZ31 at various strain rates is shown in Fig. 5 [Liu et al., 2008]. According to Fig. 5, the characteristics of magnesium alloy AZ31 stress-strain curves are represented as follows. (1) In the initial stage of the forming process, the stress abruptly increases to a peak due to the dominance of work hardening. (2) When the strain rate increases while the temperature is fixed, or the temperature decreases while the strain rate keeps unchanged, the overall level of the flow stress curve enhances correspondingly due to the growing work hardening. (3) When deformation exceeds the peak strain, the flow stress decreases at a rate which reduces with increasing strain as softening caused by DRX overtakes hardening caused by work hardening. (4) The flow stress shows steady-state region due to the equilibrium of work softening and work hardening finally. Consequently, a reasonable constitutive equation of magnesium alloy AZ31 which satisfies above deformation characteristics in the paper is adopted as follows [Liu et al., 2008],



$$\ln \sigma = \psi(\varepsilon - \varepsilon_p)^2 \ln \xi \varepsilon + \ln \sigma_p \quad (9)$$

where  $\sigma$  is plastic stress,  $\varepsilon$  is plastic strain,  $\sigma_p$  is the peak stress,  $\varepsilon_p$  is the peak strain, the value of parameter  $\xi$  is 0.6993, and the value of parameter  $\psi$  is 1.683 at the following deformation conditions: the temperature- $T$  less than or equal 523 K,  $T$  less than or equal 573K and strain rate- $\dot{\varepsilon}$  greater than or equal  $0.1s^{-1}$ ,  $T$  less than or equal 623 K and  $\dot{\varepsilon}$  greater than or equal  $1s^{-1}$ ; and the value of  $\psi$  equals to 1.28 at the other deformation conditions. The stress-strain curves of magnesium alloy AZ31 considering both macroscopic behavior and microscopic mechanism express the sensitivity of flow stress to temperature, strain rate, strain and microstructure evolution. This model of flow stress is in good agreement with the experiments data and has higher precision. The standard deviation between the model prediction values and the experiments data is approximately 2.32%. So, as far as the elevated deformation is concerned, this flow stress model can be applied to hot splitting spinning of magnesium alloy AZ31.

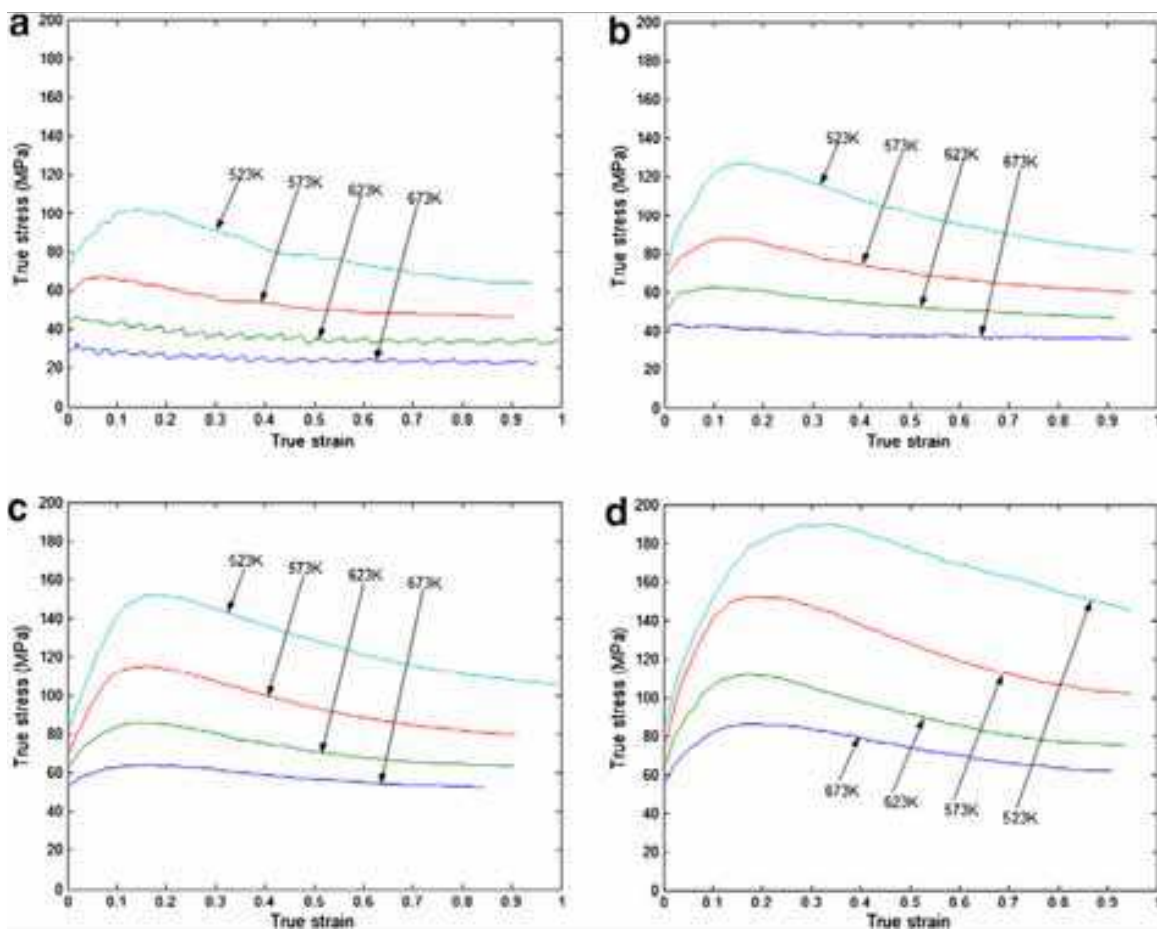


Fig. 5. Schematic of the stress-strain curves of AZ31 at various strain rates: (a)  $\dot{\varepsilon} = 0.001^{-1}$ , (b)  $\dot{\varepsilon} = 0.01^{-1}$ , (c)  $\dot{\varepsilon} = 0.1^{-1}$ , (d)  $\dot{\varepsilon} = 1^{-1}$  [Liu et al., 2008]

### 3.2.3 Application of adaptive meshing technology

For one specific problem, the determinations of the number of elements, element shapes and element types are very important in order to get more precise results based on reasonable

computational fees. During the 3D FE modeling process of hot splitting spinning of magnesium alloy AZ31, elements must own not only appreciable rigidity called anti-distorting ability, but also appreciable flexibility called good forming ability [ABAQUS (version 6.4), 2004]. Therefore, adaptive meshing technology is used to avoid the element distortion and large deformation.

Adaptive meshing technology is a tool makes it possible to maintain a high-quality mesh throughout the analysis, even when large deformation or loss of material occurs, by allowing the mesh to move independently of material. According to a comparison between distorted elements without adaptive meshing technology and normal elements with adaptive meshing technology, practical deformation can be simulated by using adaptive mesh technology [Huang<sup>1</sup> et al., 2008]. Adaptive meshing technology in ABAQUS does not change the topology of the mesh, and combines the features of pure Lagrangian analysis and pure Eulerian analysis. This type of adaptive meshing is named Arbitrary Lagrangian Eulerian (ALE) analysis.

Therefore, the FE model makes use of adaptive meshing technology in order to reduce element distortion and maintain good element aspect ratios. The domain using adaptive meshing technology is defined as Diskblank, and then the definition of the boundary smoothing region is followed that: initial feather angle is 30°, transition feather angle is also 30°, and mesh constraint angle is 60°. These settings can guarantee high computational efficiency in simulation computation. Meanwhile, in the settings of adaptive meshing technology, different remeshing frequencies may bring to different simulation results. For instance, there is almost no significant for the spinning force at different remeshing frequencies, but there is a significant deviation for the maximum equivalent plastic strain rate at different remeshing frequencies. Thus, in order to eliminate the impact on simulation results at different remeshing frequencies, the model uses remeshing sweeps after everyone increment, and define a suitable remeshing frequency.

### 3.2.4 Definition of frictional type and constraint type

The hot splitting spinning process of magnesium alloy AZ31 belongs to a continuous local plastic forming process, and the plastic forming area focuses on a small circumferential area of Diskblank. Friction behaviors during the hot forming process have particular characteristics: (1) friction between SplittingRoller and Diskblank is a main force driving the plastic forming, companying with material plastic movement, and (2) friction between flanges and exteriors of SplittingRoller or surfaces of mandrels produces along with the hot forming process, which holds back presentation of flanges and influences surface roughness of flanges. Therefore, based on the above frictional characteristics, the FE model calculates friction force by using the shear friction mode.

Constraint between mandrels and Diskblank cannot cause the plastic deformation, but may cause the elastic deformation at the beginning of the hot splitting spinning process of magnesium alloy AZ31. Diskblank rotates with mandrels, and deforms with SplittingRoller feedings. In ABAQUS, the types of constraints contain tie, rigid body, display body, coupling, shell-to-solid coupling, embedded region and equation [ABAQUS (version 6.4), 2004]. Therefore, based on above forming characteristics, one constraint called Tie is adopted to link Diskblank with mandrels due to the fact that Diskblank must rotate with mandrels. Tie can integrate mandrels with Diskblank as a whole, and provide them with different meshing methods, especially three-dimensional meshing.

### 3.3 Verification of FE model of hot splitting spinning of magnesium alloy AZ31

The FE model is reliable and reasonable based on the validation of the past research [Huang<sup>1</sup> et al., 2008]. Due to joining the thermal analysis procedure, it is necessary for hot splitting spinning of magnesium alloy AZ31 to carry out the theoretical evaluation [ABAQUS (version 6.4), 2004]. In order to indicate the FE simulation results being a receivable quasi-static solution, there are two main criteria, (1) when kinetic energy of deformation materials don't exceed approximately 5% to 10% of internal energy during the mostly simulation time, the adoptive mass scaling factor is reasonable, and (2) in order to obtain smooth solutions, it is necessary to validate whether the curve of kinetic energy is adequately smooth.

The relative values between Kinetic energy (ALLKE) and Internal energy (ALLIE) for whole model is shown in Fig. 6. According to Fig. 6, at the steady forming stage, the relative values between Kinetic energy and Internal energy is less than 5% obviously, so the curve satisfies the first criterion. The variations of Kinetic energy for whole model are shown in Fig. 7. According to Fig. 7, the Kinetic energy reaches a peak value in a short time, and then keeps steady state all the time, so the curve satisfies the second criterion. Therefore, the 3D elastic-plastic coupled thermo-mechanical FE model of hot splitting spinning of magnesium alloy AZ31 is reliable, steady and usable.

### 3.4 Characteristics of FE model

The comparisons of the modeling process between hot splitting spinning of magnesium alloy AZ31 and traditional spinning are as follows in this paper.

1. As Diskblank is extruded into the deformation zone step by step and then departs from the deformation zone after the flanges are manufactured, elastic-plastic FE method is adopted to control the elastic recovery of Diskblank in the modeling process of hot splitting spinning of magnesium alloy AZ31. But the rigid-plastic FE method is usually adopted in the modeling process of traditional spinning.
2. In the choice of FE arithmetic, a dynamic explicit algorithm in simulation of hot splitting spinning of magnesium alloy AZ31 is the same as the one in simulation of traditional spinning. The choice can avoid the characteristic of not-constringency by using a dynamic implicit algorithm.
3. In the definition of boundary conditions, since the angle between roller and blank is an important processing parameter and the roller-traces are variable, displacement boundary conditions are adopted in the definition of mechanics conditions of traditional spinning. But the angle between SplittingRoller and Diskblank is 0° and the roller-trace is unique during the hot splitting spinning process of magnesium alloy AZ31. Therefore, the velocity boundary conditions are adopted in the definition of mechanics conditions of hot splitting spinning of magnesium alloy AZ31.
4. In the element choice and meshing, triangle shell elements are usually adopted to study numerical simulations of traditional spinning, and the meshing are random. Only one element is modeled in the thickness. In this paper, due to hot splitting spinning belongs to the bulk deformation, hexahedral brick elements are adopted, which are the temperature-dependent quadratic reduced-integration elements (C3D8RT). These elements are not susceptible to locking, even when subjected to complicated states of stress. Therefore, these elements are also generally the best choice for the most general temperature-stress-displacement simulations. In meshing, concentric circle meshing mode is adopted in order to avoid hourglass modes. Furthermore, in the generation of flanges along axial direction, meshing is symmetrical.

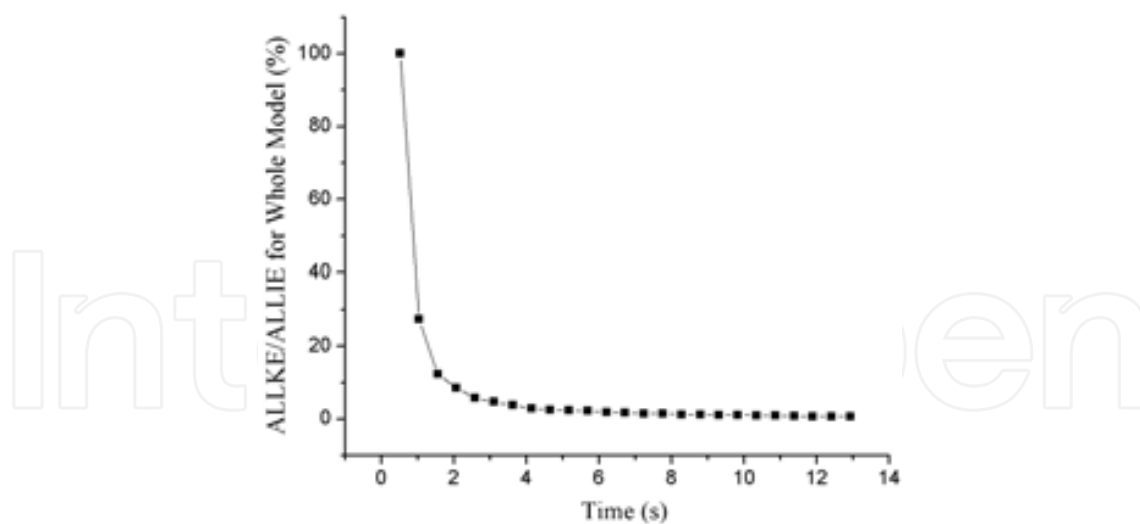


Fig. 6. The relative values between Kinetic energy and Internal energy for whole model

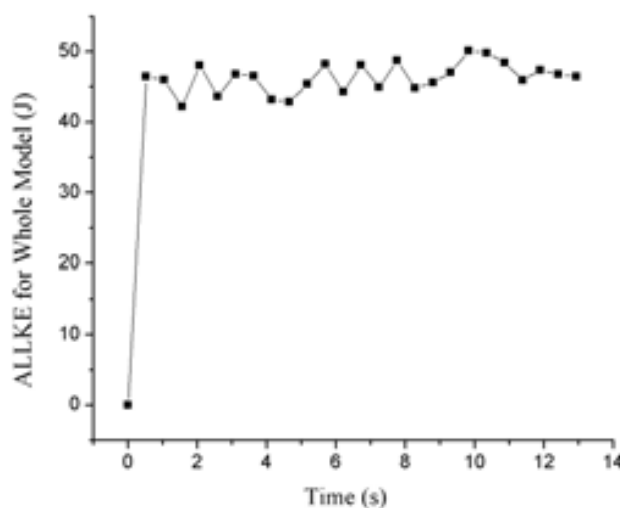


Fig. 7. The variations of Kinetic energy for whole model

#### 4. Simulation results and discussion of hot splitting spinning of magnesium alloy AZ31

Based on the above established reliable, steady and usable 3D FE model of hot splitting spinning of magnesium alloy AZ31, this study adopts the temperature-dependent thermal conductivity, thermal expansion coefficient, Young's modulus and specific heat for magnesium alloy AZ31 (density:  $1780 \text{ kg/m}^3$ , Poisson ratio: 0.33) listed in Table 1-4 [Chen, 2005; Zhang & Zhang, 2004] and processing parameters of hot splitting spinning listed in Table 5 to numerical simulate. The field distributions of deformed component, including temperature fields, stress fields and strain fields, and the variation of different nodal temperature are obtained, and the influencing laws of different initial temperatures of disk blank and different feed rates of splitting roller on the quality and precision of deformed flanges are investigated, consequently the optimal forming temperature and the optimal feed rate of splitting roller during the hot splitting spinning process of magnesium alloy AZ31 are determined.

Temperature, °C	Thermal conductivity, W/ (m·°C)
96.4	25
101	100
105	200
109	300
113	400

Table 1. Thermal conductivity of magnesium alloy AZ31

Temperature, °C	Expansion coefficient, °C <sup>-1</sup>
100	2.64E-005
200	2.7E-005
300	2.79E-005

Table 2. Thermal expansion coefficient of magnesium alloy AZ31

Temperature, °C	Young's modulus, GPa
20	40.2
75	37.3
100	34.3
125	30.9
150	30.4
200	29.4
250	27.5

Table 3. Young's modulus of magnesium alloy AZ31

Temperature, °C	Specific Heat, J (kg·°C)
20	1050
100	1130
200	1170
300	1210
350	1260

Table 4. Specific Heat of magnesium alloy AZ31

Initial diameter of Diskblank, mm	100.0
Initial thickness of Diskblank, mm	10.0
Diameter of SplittingRoller, mm	99.17
Splitting angle of SplittingRoller, degree	45.0
Radius of corner of SplittingRoller, mm	1.0
Feed rate of SplittingRoller, mm/ s	1.0
Rotational speed of Mandrels, rpm	98.0
Dimension of Mandrels, mm	100.0
Friction coefficient between Diskblank and SplittingRoller	0.15
Friction coefficient between Diskblank and Mandrels	0.15
Temperature of environment, °C	20
Temperature of dies, °C	200
Initial temperature of Diskblank, °C	300
Heat transfer coefficient (Diskblank-dies), W/ (m <sup>2</sup> ·C)	2000
Heat transfer coefficient (Diskblank-environment), W/ (m <sup>2</sup> ·C)	20

Table 5. Processing parameters of hot splitting spinning

#### 4.1 Temperature fields

During the hot splitting spinning process of magnesium alloy AZ31, because of the heat exchange between Diskblank and the external environment or the heat loss and the uneven interior heat source caused by the inhomogeneous deformation of Diskblank, the inner temperature gradient of deformed Diskblank are very large. Temperature field distributions of Diskblank during the process are shown in Fig. 8. According to Fig. 8, temperature field distributions of Diskblank are very uneven, and the temperature of deformed section of Diskblank is much higher than that of undeformed section. The temperature of inner section of Diskblank contacting with roller is higher than that of bilaterally symmetrical sections of Diskblank contacting with mandrels. The former temperature reaches about 270°C and the latter temperature is just about 220°C, as shown in Fig. 8(a), and the former temperature reaches about 250°C and the latter temperature is just about 210°C, as shown in Fig. 8(b). It is because friction and plastic deformation produce heat during the process, but the type of contact is surface contact and the temperature difference between dies and Diskblank is relatively large, so as to appear the large temperature gradients.

#### 4.2 Nodal temperatures

In order to study the variations of different nodal temperatures for the whole disk blank, the location of trace points, including point A, point B and point C in the middle layer of disk blank and point D, point E and point F in the upper layer of disk blank, are shown in Fig. 9. The variations of temperatures with time at different trace points during the process are

shown in Fig. 10. From Fig. 10, the temperature variations between point A and point D is similar, so do point B and point E as well as point C and point F. Point A and point D are both the trace points of outer circumferential surface of disk blank, but point A contacting with roller in the middle layer belongs to local plastic deformation zone and point D contacting with mandrels in the upper layer belongs to deformed flanges zone. Although the curves between point A and point D are similar, the temperature of point A reaches one extremum at intervals at the ending stage of the process and the extremum is a little more than that of point D. Because at the ending stage of the process, the deformation heat leads to ascend at intervals at point A after the temperature of point A goes down to about 240°C. Besides, point A obtains the contact heat, radiation and friction heat, so that the temperature of point A is more than that of point D. Because of higher temperature of Diskblank, heat exchange exists between dies and environment. There is no enough time to exchange heat with the outside at the beginning of simulation, but as the simulation going on, external temperature of Diskblank descends, so there is a temperature gradient between inside and outside of Diskblank leading to the heat is transferred to the outside of Diskblank.

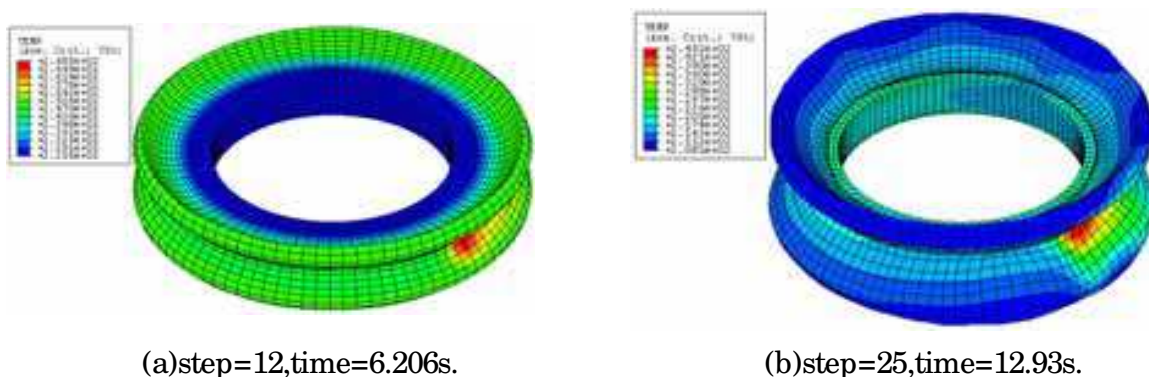


Fig. 8. Temperature field distributions of Diskblank

The curve of point B is extremely similar to the curve of point E and the curve of point C is also extremely similar to the curve of point F, but the temperature of point B is a little more than that of point E and the temperature of point C is a little more than that of point F. The point in the middle layer of disk blank lies on the local plastic deformation zone, so more deformation heat is obtained. For the temperature distributions in the same layer of disk blank, the temperature of point A is more than that of point B and the temperature of point B is more than that of point C, and meanwhile the temperature of point D is more than that of point E and the temperature of point E is more than that of point F. The reasons are that, the deformation of outside circumferential zone is larger, and meanwhile the deformation energy and friction heat is larger than heat transferred from the surface to the environment. So, the temperature of point A and that of point D are relatively higher.

#### 4.3 Strain fields

The logarithmic strain vector distributions at the ending stage of deformation are shown in Fig. 11. The logarithmic strain can reflect the accumulative effects of plastic deformation and metal flow directions. Therefore, the upper surface of deformed flanges contacting with mandrels and the under surface of deformed flanges contacting with roller both perform the tensile stress during the hot splitting spinning process of magnesium alloy AZ31, including

section A and section C, as shown in Fig. 11. This state leads to the increase of deformed flanges steadily. But Diskblank in section A and section C will fracture on condition that larger tensile stress. The middle part of deformed flanges performs the compressive stress during the process, including section B, as shown in Fig. 11. This state leads to deformed flanges being more regular figures and higher quality and precision. But Diskblank in section B will wrinkle on condition that larger compressive stress.

The variations of equivalent plastic strain fields with time during the hot splitting spinning process of magnesium alloy AZ31 are shown in Fig. 12. Compared with the past research on cold splitting spinning [Huang<sup>1</sup> et al., 2008], the temperature of two flanges is higher than that of local plastic deformation zone of flanges during the process due to deformed flanges

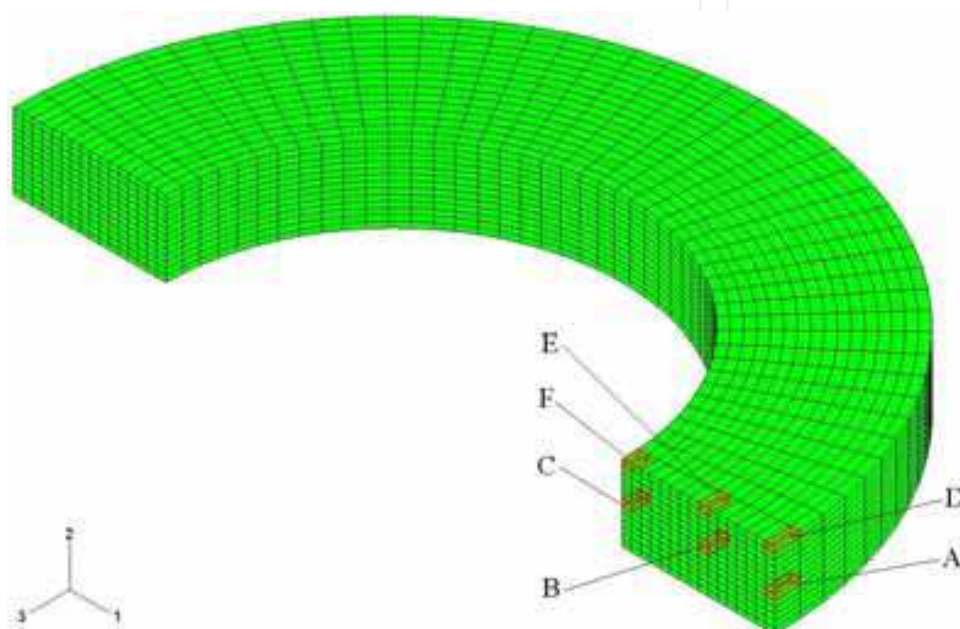


Fig. 9. Location of trace points

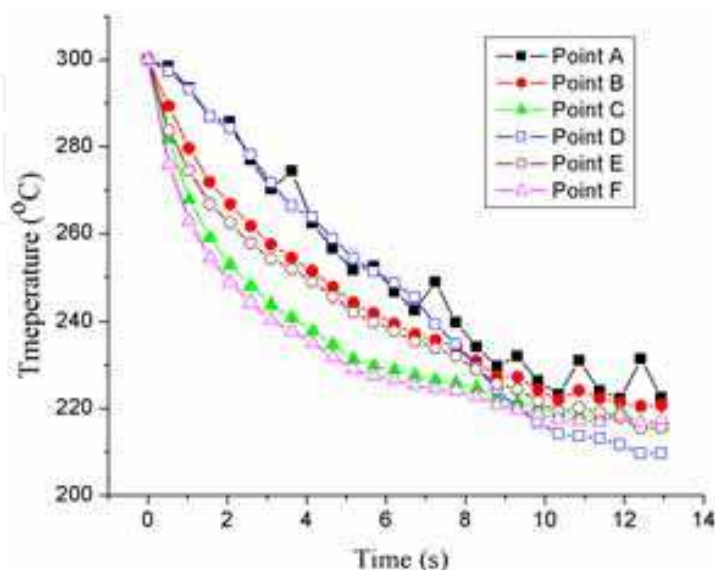


Fig. 10. Variations of temperatures with time at different trace points



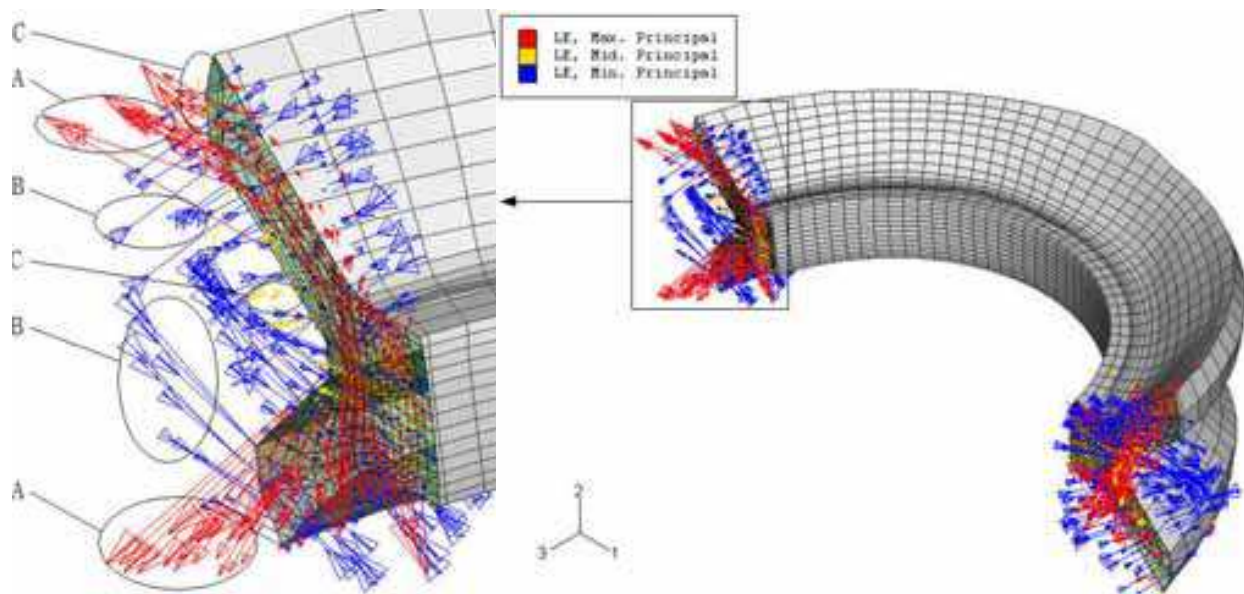


Fig. 11. Logarithmic strain vector distributions at the ending stage of deformation: A-Red, B-Blue, C-Yellow

contacting with both roller and mandrels. Consequently, there are two symmetrical belts in which equivalent strain distributions are uniform and even, as shown in Fig. 12(b). Furthermore, due to the thermal plastic deformation, the maximum equivalent plastic strain of hot splitting spinning is more than the maximum equivalent plastic strain of cold splitting spinning.

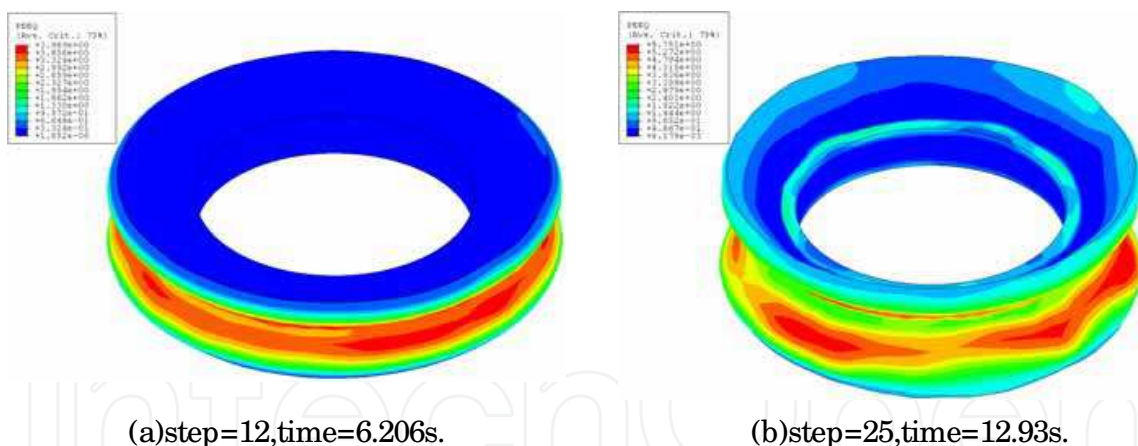


Fig. 12. The variations of equivalent plastic strain fields with time

#### 4.4 Stress fields

The variations of equivalent stress fields with time during the hot splitting spinning process of magnesium alloy AZ31 are shown in Fig. 13. From Fig.13, compared with the past research on cold splitting spinning [Huang<sup>1</sup> et al., 2008], stress concentration are not presented in the local plastic deformation zone contacting with roller due to the existence of softening process from DRX. There are enough heat for DRX in the upper surface of disk blank, therefore stress concentration are presented in the zone contacting with mandrels. Furthermore, the figure of stress concentration zone isn't like a belt, only a corresponding section contacting with local plastic deformation zone.

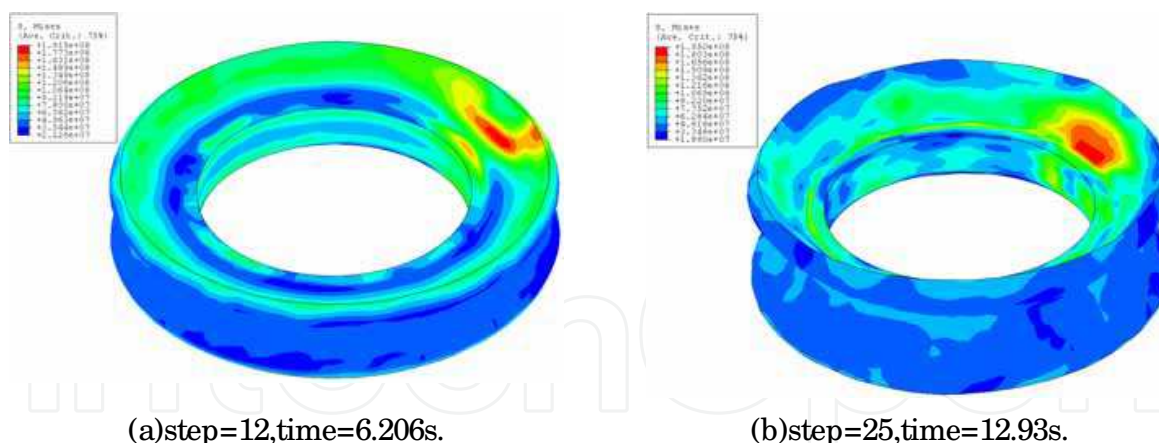


Fig. 13. The variations of equivalent stress fields with time

#### 4.5 Forming quality of deformed flanges

Due to the existence of softening process from DRX, different initial temperatures of disk blank and different feed rates of splitting roller have the important effects on the forming quality and precision of deformed flanges, so the corresponding influencing laws must be investigated. To study of the influencing laws of different initial temperatures of disk blank and different feed rates of splitting roller on the forming quality and precision of deformed flanges, the quantitative evaluations of deformed flanges are as following [Huang et al., 2009], including thickness deviation of flanges -  $\delta_t$  and angle deviation of inner-face/ outer-face -  $\delta_1 / \delta_2$ . The definition of the responding geometries of roller and disk blank is shown in Fig. 14. The thickness deviation of flanges -  $\delta_t$  is expressed by

$$\delta_t = \frac{t - t_0}{t_0} \times 100\% \quad (10)$$

where  $t$  is the thickness of simulation results and  $t_0$  is the standard thickness. The angle deviation of inner-face -  $\delta_1$ , which contacts with the surfaces of roller, is expressed by

$$\delta_1 = \frac{\alpha_1 - \alpha_0}{\alpha_0} \times 100\% \quad (11)$$

where  $\alpha_1$  is the angle of inner-face of flanges and  $\alpha_0$  is the standard angle. The angle deviation of outer-face -  $\delta_2$ , which contacts with the surfaces of mandrels, is expressed by

$$\delta_2 = \frac{\alpha_2 - \alpha_0}{\alpha_0} \times 100\% \quad (12)$$

where  $\alpha_2$  is the angle of outer-face of flanges.

The influencing laws of initial temperature of Diskblank on thickness deviation of deformed flanges are shown in Fig. 15. From Fig. 15, in the defined scope of initial temperature of Diskblank, thickness deviation of deformed flanges decreases distinctly at the beginning stage, and then is close to approximately zero when temperature is 300°C, and increases gradually with the increase of forming temperature, and finally reaches about 2%.

The influencing laws of initial temperature of Diskblank on angle deviation of deformed flanges are shown in Fig. 16. From Fig. 16, in the defined scope of initial temperature of Diskblank, the angle deviation of outer-face is a little more than that of inner-face, and they remain with the similar curves. The curves decrease distinctly at the beginning stage, and then increase gradually with the increase of forming temperature. When temperature is 300°C, both angle deviations of deformed flanges are close to approximately zero simultaneously.

The influencing laws of feed rate of splitting roller on thickness deviation of deformed flanges are shown in Fig. 17. From Fig. 17, in the defined scope of feed rate of splitting roller, there are three phases for the changing curve. When  $v < 1$  mm/s, thickness deviation of deformed flanges increases distinctly and is negative. When  $1 \leq v \leq 3$  mm/s, thickness deviation holds approximately zero. When  $v > 3$  mm/s, thickness deviation increases gradually and are positive, and the value is more than 4%.

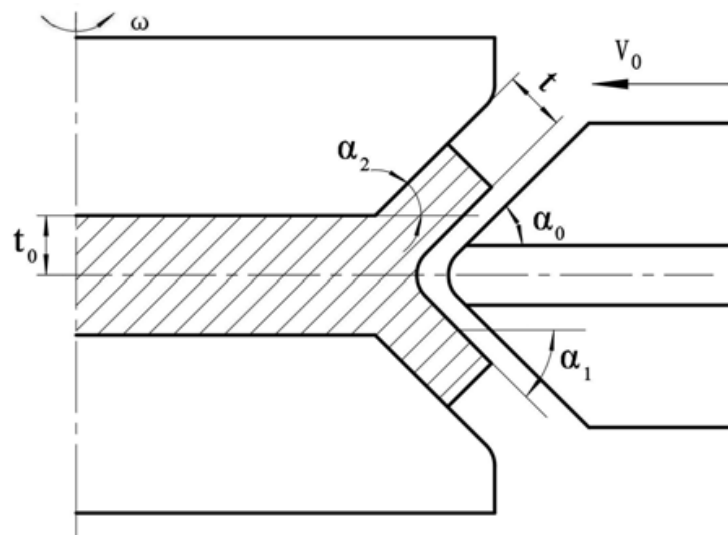


Fig. 14. The definition of the responding geometries of roller and disk blank

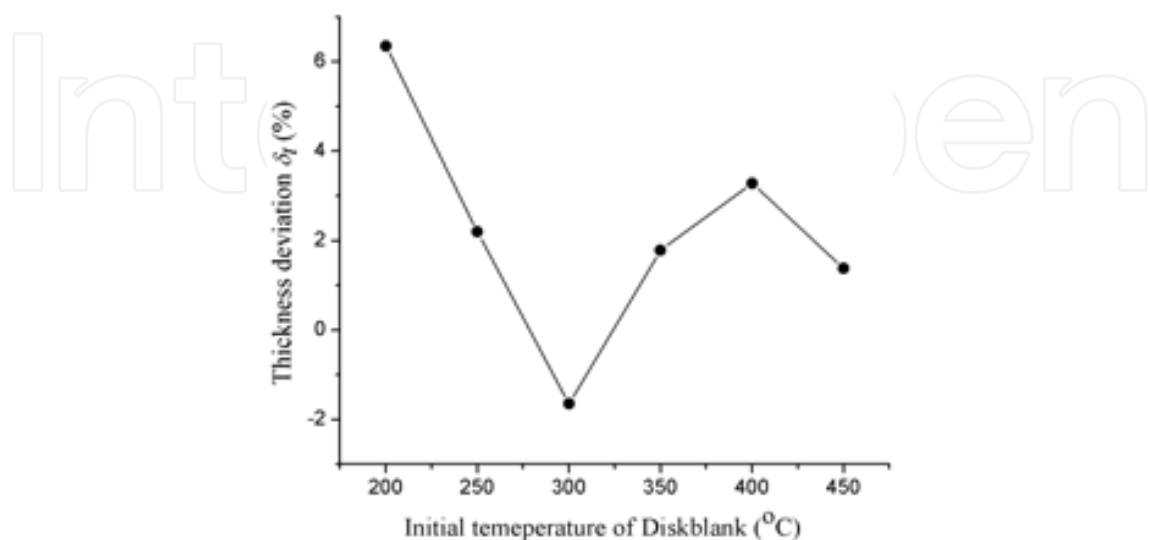


Fig. 15. The influencing laws of initial temperature of Diskblank on thickness deviation

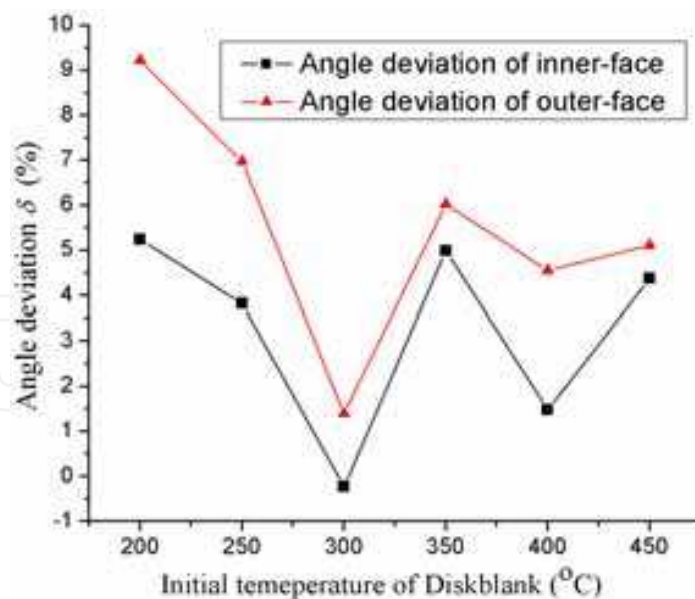


Fig. 16. The influencing laws of initial temperature of Diskblank on angle deviation

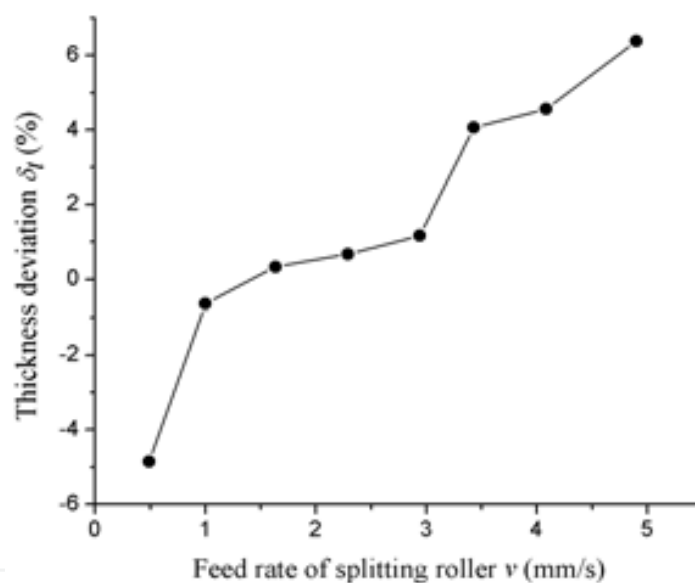


Fig. 17. The influencing laws of feed rate of splitting roller on thickness deviation

The influencing laws of feed rate of splitting roller on angle deviation of deformed flanges are shown in Fig. 18. From Fig. 18, in the defined scope of feed rate of splitting roller, when  $v < 1$  mm/s, angle deviation of deformed flanges increases suddenly and are negative, and the values are less than  $-8\%$ ; when  $1 \leq v \leq 3$  mm/s, angle deviation hold approximately from 0 to 2%; when  $v > 3$  mm/s, angle deviation increases gradually, and angle deviation of inner-face reaches above 2% and angle deviation of outer-face reaches above 4%.

The above two quantitative evaluations of deformed flanges are relatively larger values when temperature is about  $200^\circ\text{C}$ , namely, for initial temperature of Diskblank, thickness deviation is more than 6%, angle deviation of inner-face is more than 9% and angle deviation of outer-face is more 5%, and meanwhile for feed rate of splitting roller, thickness deviation is less than  $-5\%$ , angle deviation of inner-face and outer-face are both less than

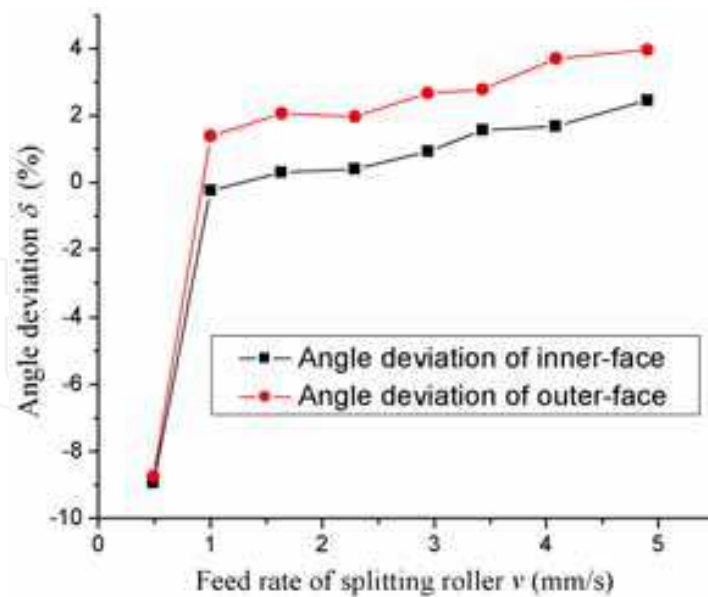


Fig. 18. The influencing laws of feed rate of splitting roller on angle deviation

-9%. And when temperature is about 450°C, the above two quantitative evaluations of deformed flanges become even and steady, but larger values, namely, for initial temperature of Diskblank, thickness deviation is more than 4%, angle deviation of inner-face is more than 6% and angle deviation of outer-face is more 5%, and meanwhile for feed rate of splitting roller, thickness deviation is more than 6%, angle deviation of inner-face and outer-face are both less than 4%. Only when forming temperature is about 300°C, the above two quantitative evaluations of deformed flanges are close to zero. The reasons are that, strain hardening and softening from DRX keeps an appropriate balance during the hot splitting spinning process of magnesium alloy AZ31 when temperature is about 300°C, so here thickness deviation is minor and angle deviation is close to zero, and forming quality and precision are highest. In the same way, when the feed rate of splitting roller is defined from 1 to 3mm/ s, forming quality and precision are also highest during the hot splitting spinning process of magnesium alloy AZ31. Consequently, the optimal forming temperature is approximate 300°C and the optimal feed rate of splitting roller ranges from 1 to 3mm/ s during the hot splitting spinning process of magnesium alloy AZ31.

## 5. Conclusions

In this paper, hot forming characteristics of magnesium alloy AZ31 are analyzed and a reasonable deformation temperature range is obtained during the thermoplastic forming process. Based on the FEM software platform of ABAQUS/ Explicit and a developed three-dimensional FE model of cold splitting spinning, a three-dimensional elastic-plastic FE model of hot splitting spinning of magnesium alloy AZ31 is established, and the forming characteristics and laws are as follows.

1. During the hot splitting spinning process of magnesium alloy AZ31, temperature field distributions of Diskblank are very uneven, and the temperature of inner section of Diskblank contacting with roller is higher than that of bilaterally symmetrical sections of Diskblank contacting with mandrels, so there is a temperature gradient between inside and outside of Diskblank.

2. During the process, section A and section C (Fig. 11) perform the tensile stress, and this state leads to the increase of deformed flanges steadily; section B (Fig. 11) performs the compressive stress, and this state leads to deformed flanges being more regular figures and higher quality and precision. There are two symmetrical uniform belts in the equivalent strain distributions, and the stress concentration is presented in only one section contacting with mandrels.
3. The optimal forming temperature is approximate 300°C and the optimal feed rate of splitting roller ranges from 1 to 3mm/ s during the hot splitting spinning process of magnesium alloy AZ31.

## 6. Acknowledgements

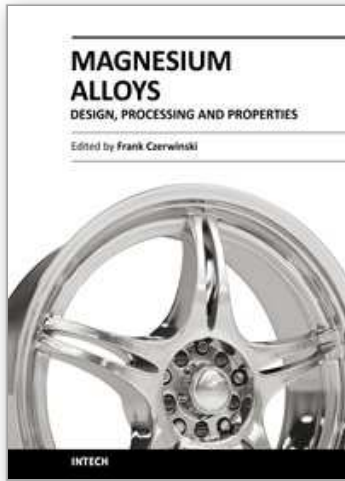
The authors would like to thank the National Natural Science Foundation of China (Nos. 50405039 and 50575186), the National Science Found of China for Distinguished Young Scholars (No. 50225518), the National "863" Project of China (No. 2008AA04Z122) and the Foundation of NWPU (No. W018104) for the support given to this research.

## 7. References

- ABAQUS (version 6.4) (2004). ABAQUS Analysis User's Manual, Inc.
- Chen Zhenhua (2005). *Deformation Magnesium Alloys*, Chemical Industry Press, Beijing (in Chinese)
- Chino<sup>1</sup> Yasumasa, Kimura Katsuya, Hakamada Masataka & Mabuchi Mamoru (2008). Mechanical anisotropy due to twinning in an extruded AZ31 Mg alloy, *Mater. Sci. Eng. A*, 485, 311–317
- Chino<sup>2</sup> Yasumasa, Kimura Katsuya & Mabuchi Mamoru (2008) Twinning behavior and deformation mechanisms of extruded AZ31 Mg alloy, *Mater. Sci. Eng. A*, 486, 481–488
- Doege E. & Droder K. (2001). Sheet metal forming of magnesium wrought alloys — formability and process technology, *J Mater. Process. Technol.*, 115, 14–19
- Grass H., Kremaszky C., Reip T. & Werner E. (2003). 3-D Simulation of hot forming and microstructure evolution, *Comput. Mater. Sci.*, 28, 469–477
- Grass H., Kremaszky C. & Werner E. (2006). 3-D FEM-simulation of hot forming processes for the production of a connecting rod, *Comput. Mater. Sci.*, 36, 480–489
- Hauk Stefan, Vazquez Victor H. & Altan Taylan (2000). Finite element simulation of the Flow-Splitting-Process, *J Mater. Process. Technol.*, 98, 70–80
- Huang<sup>1</sup> Liang, Yang He & Zhan Mei (2008). 3D-FE modeling method of splitting spinning, *Comput. Mater. Sci.*, 42, 643–652
- Huang<sup>2</sup> Liang, Yang He, Zhan Mei & Hu Li-jin (2008). Numerical simulation of influence of material parameters on splitting spinning of aluminum alloy, *Trans. Nonferrous Met. Soc. China*, 18, 674–681
- Huang<sup>3</sup> Liang, Yang He, Zhan Mei & Yuli Liu (2008). Analysis of splitting spinning force by the principal stress method, *J Mater. Process. Technol.*, 201, 267–272
- Huang Liang, Yang He, Zhan Mei & Lijin Hu (2009). Forming characteristics of splitting spinning based on the behaviors of roller, *Comput. Mater. Sci.*, 45, 449–461

- Liu Juan, Cui Zhenshan & Li Congxing (2008). Modelling of flow stress characterizing dynamic recrystallization for magnesium alloy AZ31B, *Comput. Mater. Sci.* 41, 375–382
- Michael M. , Avedesian & Baker, Hugh (1999). *Magnesium and Magnesium Alloys*, ASM Specialty Handbook, USA
- Mordike B. L. & Ebert T. (2001). Magnesium Properties — applications — potential, *Mater. Sci. Eng. A*, 302, 37–45
- Ogawa N., Shiomi M. & Osakada K. (2002). Forming limit of magnesium alloy at elevated temperatures for precision forging, *Int. J Mach. Tools Manuf.*, 42, 607–614.
- Palumbo G., Sorgente D., Tricarico L., Zhang S. H. & Zheng W. T. (2007). Numerical and experimental investigations on the effect of the heating strategy and the punch speed on the warm deep drawing of magnesium alloy AZ31, *J Mater. Process. Technol.*, 191, 342–346
- Schmoeckel Dieter & Hauk Stefan (2000). Tooling and process control for splitting of disk blanks, *J Mater. Process. Technol.*, 98, 65–69
- Song Y. H., Zhang K. F., Wang Z. R. & Diao F. X. (2000). 3-D FEM analysis of the temperature field and the thermal stress for plastics thermalforming, *J Mater. Process. Technol.*, 97, 35–43
- Staroselsky A. & Anand L. (2003). A constitutive model for hcp materials deforming by slip and twinning: application to magnesium alloy AZ31B, *Int. J Plast.*, 19, 1843–1864
- Wang Chenghe & Liu Kezhang (1986). *Spinning Technology*, China Machine Press, Beijing (in Chinese)
- Wong C. C., Dean T. A. & Lin J (2003). A review of spinning, shear forming and flow forming process, *Int. J Mach. Tools Manuf.*, 43, 1419–1435
- Yang H., Zhan M., Liu Y. L., Xian F. J, Sun Z. C., Lin Y. & Zhang X. G. (2004). Some advanced plastic processing technologies and their numerical simulation, *J Mater. Process. Technol.*, 151, 63–69
- Yu Hanqing & Chen Jnde (1999). *The principle of metal plastic forming*, China Machine Press, Beijing (in Chinese)
- Zhang Jn & Zhang Zonghe (2004). *Magnesium Alloy and Its Application*, Chemical Industry Press, Beijing (in Chinese)

IntechOpen



## **Magnesium Alloys - Design, Processing and Properties**

Edited by Frank Czerwinski

ISBN 978-953-307-520-4

Hard cover, 526 pages

**Publisher** InTech

**Published online** 14, January, 2011

**Published in print edition** January, 2011

Scientists and engineers for decades searched to utilize magnesium, known of its low density, for light-weighting in many industrial sectors. This book provides a broad review of recent global developments in theory and practice of modern magnesium alloys. It covers fundamental aspects of alloy strengthening, recrystallization, details of microstructure and a unique role of grain refinement. The theory is linked with elements of alloy design and specific properties, including fatigue and creep resistance. Also technologies of alloy formation and processing, such as sheet rolling, semi-solid forming, welding and joining are considered. An opportunity of creation the metal matrix composite based on magnesium matrix is described along with carbon nanotubes as an effective reinforcement. A mixture of science and technology makes this book very useful for professionals from academia and industry.

### **How to reference**

In order to correctly reference this scholarly work, feel free to copy and paste the following:

He Yang, Liang Huang and Mei Zhan (2011). Hot Forming Characteristics of Magnesium Alloy AZ31 and Three-Dimensional FE Modeling and Simulation of the Hot Splitting Spinning Process, *Magnesium Alloys - Design, Processing and Properties*, Frank Czerwinski (Ed.), ISBN: 978-953-307-520-4, InTech, Available from: <http://www.intechopen.com/books/magnesium-alloys-design-processing-and-properties/hot-forming-characteristics-of-magnesium-alloy-az31-and-three-dimensional-fe-modeling-and-simulation>

**INTECH**  
open science | open minds

#### **InTech Europe**

University Campus STeP Ri  
Slavka Krautzeka 83/A  
51000 Rijeka, Croatia  
Phone: +385 (51) 770 447  
Fax: +385 (51) 686 166  
[www.intechopen.com](http://www.intechopen.com)

#### **InTech China**

Unit 405, Office Block, Hotel Equatorial Shanghai  
No.65, Yan An Road (West), Shanghai, 200040, China  
中国上海市延安西路65号上海国际贵都大饭店办公楼405单元  
Phone: +86-21-62489820  
Fax: +86-21-62489821



© 2011 The Author(s). Licensee IntechOpen. This chapter is distributed under the terms of the [Creative Commons Attribution-NonCommercial-ShareAlike-3.0 License](#), which permits use, distribution and reproduction for non-commercial purposes, provided the original is properly cited and derivative works building on this content are distributed under the same license.

IntechOpen

IntechOpen